

Synthesis and electrorheological characteristics of microencapsulated polyaniline particles with melamine–formaldehyde resins

Y.H. Lee^a, C.A. Kim^a, W.H. Jang^a, H.J. Choi^{a,*}, M.S. Jhon^b

^aDepartment of Polymer Science and Engineering, Inha University, Incheon 402-751, South Korea

^bDepartment of Chemical Engineering, Carnegie Mellon University, Pittsburgh, PA 15213, USA

Received 6 December 2000; received in revised form 8 February 2001; accepted 23 March 2001

Abstract

Polyaniline particles with low pH cannot be directly used in the electrorheological (ER) systems, since their emerald base form has a conductivity that is too high. Therefore, the pH of the polyaniline has been controlled to yield a lower conductivity. To improve the particle preparation method for polyaniline, which generates ER fluids with its semi-conducting characteristics, we synthesized microencapsulated polyaniline particles with melamine–formaldehyde (MF) resins. Microcapsules, containing polyaniline with a low pH as the core material, were prepared by polymerization of MF resin, which play the role of an insulator between the polyaniline particles. From rheological measurements, the yield stress of the ER fluid decreased with the increase of MF resin, and this effect enhanced as the applied electric field strength increased. © 2001 Published by Elsevier Science Ltd.

Keywords: Microencapsulation; Polyaniline; Electrorheological fluid

1. Introduction

Electrorheological (ER) fluids, composed of electrically polarizable materials dispersed in a low dielectric base fluid, have recently been investigated, because their technical applications are very promising [1]. These fluids represent a unique class of electroactive materials that exhibit modified flow properties under imposed AC or DC electric fields. The influence of the electric fields on the deformation and flow properties of ER materials has been of interest for many years. When an electric field is imposed, particles in the fluid form fibrillation structures, which are oriented along the direction of the electric field. These chains are held together by interparticle forces, which have sufficient strength to inhibit fluid flow. Therefore, a stress is required to break the chainlike (or columnar) structures, and this stress, referred to as yield stress, can be described by the Bingham plastic model [2]. When the electric field is removed, the particles return to an original random orientational distribution, and the suspension behaves like Newtonian fluid. Thereby, controllable viscosity, fast response, and the simplicity of engineering designs using ER fluids have facilitated the development of many devices,

such as active engine mounts, shock absorbers, and adaptive structures [3].

Among various dry base ER fluids, such as PZT [4], carbonaceous particles [5], zeolite [6,7], and phosphate cellulose [8], ER materials have recently focused on conjugated polymer particles, because their application is particularly interesting due to the fact that such typical drawbacks of conductive polymers (moderate conductivity, powder form, and insolubility) become advantages for ER applications [9–13]. They further provide flexibility; their physical and chemical properties can be tailored to maximize the ER effect. Therefore, some semi-conducting materials have been used as substrates for anhydrous ER suspensions. One of the most extensively studied materials in this category is polyaniline (PANI), which has been examined for ER behavior [14,15]. PANI in its emeraldine base form has advantages with respect to density, conductivity control, and thermal stability. We have extensively studied the ER properties of anhydrous suspensions based on PANI, such as homopolymers [16,17], poly(aniline-*co*-*o*-ethoxyaniline) [18,19], poly(aniline-*co*-sodium diphenylamine sulfonate) [20,21], and polyaniline–clay nanocomposites [22,23].

In fact, to obtain semi-conducting PANI for ER materials, the polyaniline particles must be dedoped by reducing the pH of the aqueous medium. Additional doping and dedoping steps are needed to control the conductivity of the particles

* Corresponding author. Tel.: +82-32-860-7486; fax: +82-32-865-5178.
E-mail address: hjchoi@inha.ac.kr (H.J. Choi).

for improved ER performance. A simple protonic acid treatment can alter the PANI properties from conducting to insulating [24]. This allows for a change in both the dielectric constant and conductivity of particles while keeping all other particle properties the same. Contrary to this conventional conductivity control, we adopt a microencapsulation technique to control the conductivity of the polyaniline particles in this paper. For the modified PANI-based ER fluids, Akhavan et al. [25] reported coating PANI particles with insulating polymer to improve ER efficiency.

Microencapsulation is a well-known process in which tiny particles or droplets are covered by a coating or a membrane. The microencapsulation concept originally was used in the ink formulations for carbonless copy paper and has been successfully applied for various areas, including the pharmaceutical and biomedical industries [26]. The main purpose for adopting the microencapsulation method is to control the conductivity of the ER fluid without doping and dedoping steps, which are very time consuming. The pH of the PANI particles is critical to the ER efficiency and microencapsulation requires a relatively short reaction, compared to the doping and dedoping process. Microencapsulation is also able to easily produce diverse microcapsules by controlling reaction parameters. Among various shell materials for microcapsules, amino resins (more precisely urea and/or melamine–formaldehyde (MF) resins) play an important role [27–29]. The raw materials are inexpensive and easy to obtain.

Compounds with NH groups can react with aldehydes and ketones to form additional condensation products. Examples of these reactions are the condensations of urea and melamine with formaldehyde [30]. Because MF resins are known to be superior to urea–formaldehyde resins in hardness and heat and water resistance, they are suitable for microencapsulation of the homopolyaniline particles. Using synthesized encapsulated polyaniline particles, we investigated the ER properties as functions of electric field strength, shear rate, and encapsulation condition.

2. Experimental

2.1. Synthesis of polyaniline

PANI particles were synthesized using the conventional oxidation polymerization of aniline to produce a fine emeraldine hydrochloride form [31]. A solution of 1.2 mol aniline monomer in 800 ml of 1 M HCl was chilled and stirred for 2 h, and polymerization was initiated at -5°C by a pre-chilled solution of 0.72 mol ammonium peroxy-sulfate in 400 ml of 1 M HCl. The reaction was maintained for an additional 2 h to complete the reaction to produce the emeraldine hydrochloride form of PANI. A small amount of 1 M NaOH was finally injected into the reactor to precipitate the PANI particles. After washing with distilled water several times and measuring the pH, this precipitate was

filtered and washed with distilled water and ethanol to remove the unreacted monomer and oligomer. Products were dried for 1 day using a freeze-drying process.

2.2. Preparation of microcapsules

Synthesized PANI particles were used as the core material for the encapsulation, and prepolymer MF as the shell materials. A mixture of 25 g of 20% citric acid and 100 g of distilled water was prepared. The pH of this solution is titrated to 4 with 1 M NaOH. A quantity of 10 g, which is fixed for all experiments, of PANI particles were then added to this solution. After stirring this mixed solution for 2 h at $40\text{--}45^{\circ}\text{C}$ in a water bath, the melamine prepolymer and formaline (37% formaldehyde) was added while stirring.

As the temperature rose to approximately 65°C , the MF resins were cured [32,33], and microencapsulated polyaniline (MCPA) particles were produced. After completion of the encapsulation reaction, the particles were filtered and washed with distilled water several times to remove the unreacted chemicals. Finally, the products were dried in a vacuum oven [34]. Note that the polyaniline particles also require time consumption on sample preparation of the ER fluids due to both a polymerization of monomer and an after-treatment of the synthesized particle such as washing, filtering and drying. Encapsulated PANI samples were further prepared by varying the content of MF with a fixed molar ratio of melamine to formaldehyde; the ratios for MCPA1, MCPA2, and MCPA3 were 45 g:69 g, 60 g:92 g, and 75 g:115 g, respectively.

2.3. Characterization

A Fourier Transform Infrared spectrometer (FT-IR, Perkin Elmer System 2000, Norwalk, CT) was used to identify the chemical structure of the solid MCPA specimens, which were prepared by grinding the powder sample with KBr. The MCPA samples were compared with the spectrum of PANI sample reported. Thermal stability of MCPA particles was examined by using thermogravimetric analyzer (TGA, Polymer Laboratories, PL-TGA, Amherst, MA) at a heating rate of $10^{\circ}\text{C}/\text{min}$ from 25 to 600°C . The shape of the MCPAs was also observed using a scanning electron microscope (SEM, S-4200, Hitachi, Hitachnaka-shi, Japan), with a magnification of 600 and 7000 at 10 kV. Particle size distribution and average size of the MCPAs were also measured using a laser particle analyzer (MALVERN MS 20, Malvern, UK).

Conductivities of PANI and MCPA particles were measured from a two-probe method using compressed disks, which were prepared using a 13 mm KBr pellet die. The resistance of the pellet was measured by a picoammeter (Keithley model 485, Cleveland, OH) with a conductivity cell [35]. ER fluids were prepared by dispersing the powdery MCPAs in dry silicone oil with 20 wt% solid content. The density and kinematic viscosity of the silicone oil were $0.95\text{ g}/\text{cm}^3$ and 50 cS, respectively. For the fixed

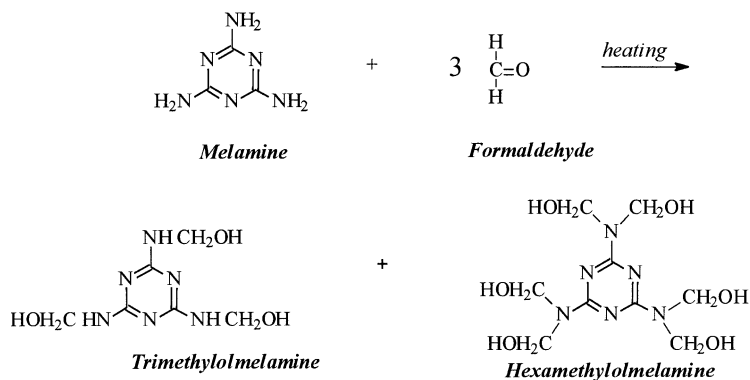
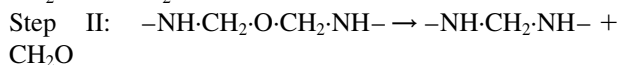
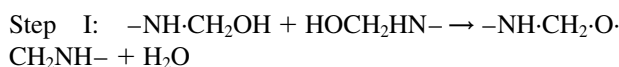


Fig. 1. Mechanism for polymerization of MF resin.

particle concentration of 20 wt%, ER properties were examined via a rotational rheometer (Physica MC 120, Stuttgart, Germany), with a Couette-type geometry equipped with a high voltage generator (Physica HVG 5000, Stuttgart, Germany). Note that the rheological measurement with different geometries such as squeezing flow [36] and vertical oscillation flow [37] has been also investigated. The suspension was placed in the gap between the stationary outer measuring cup and the rotating measuring bob. The HVG 5000 could supply DC voltages up to 5 kV with $\pm 10 \mu\text{A}$ of electric current. Various static DC electric fields were applied to the cylindrical cup, perpendicular to the flow direction: the inner wall of the cup was the anode, and the bob was the cathode. To obtain an equilibrium internal structure of the particles, an electric field was applied to the ER fluids for 3 min before the rheological measurements were recorded. All measurements were taken at 25°C unless specified.

3. Results and discussion

Reaction between melamine and formaldehyde at 65°C leads to tri- and hexa-methylolmelamine as shown in Fig. 1. Further heating condenses the methylolmelamines, and precipitates the resin. In this reaction, methylol condensation and the building of methylene bridges follow successively, as shown in the following two-step reaction.



Note that the capsule content, termed the ‘internal phase’, is solid PANI.

Fig. 2 shows the FT-IR spectra for the MCPA particles. The peaks at 1480, 1550 and 3300, 1363, and 1660 cm^{-1} indicate $-\text{CH}_2-$, N–H, C–N, and C=N, respectively. These spectra indicate that MCPA was successfully synthesized using MF resins. Note that PANI has peaks at 824, 1144

and 1309, and 1490 and 1586 cm^{-1} indicating aromatic C–H, aromatic amine, and aromatic C–C stretching vibrations [21].

Fig. 3(a) and (b) shows SEM photographs of both PANI particles and MCPA3 particles. The shape of MCPA from the SEM photograph was grape-like [34]. With respect to the shape and size, the MCPA was observed to be larger and more spherically symmetric than the PANI, which has an average particle size of 17.9 μm . The average particle sizes of MCPA1, MCPA2 and MCPA3 are 48.1, 57.6 and 86.4 μm , respectively. The particle size distribution shifts toward larger sizes by increasing the content of MF resin as shown in Fig. 4. All these measurements suggest that the thickness of the MF coating wall increases with the resin amount.

Fig. 5 shows TGA diagram of the PANI and MCPA particles. The thermogram indicates that the weight loss around 100°C was due to evaporation of water or solvent used for washing, and decomposition of the PANI particle began at approximately 350°C. Weight loss of this sample was approximately 20% at 600°C, showing that the prepared PANI particles have a good thermal stability. Kulkarni et al. [38] investigated thermal stability of PANI and suggested that the decomposition of the doped PANI was described as a two-step process. The first step is the loss of the dopant and

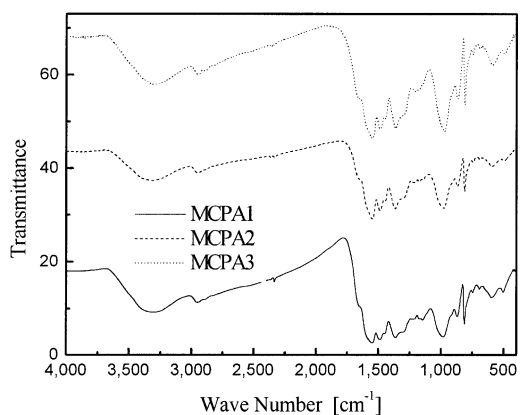
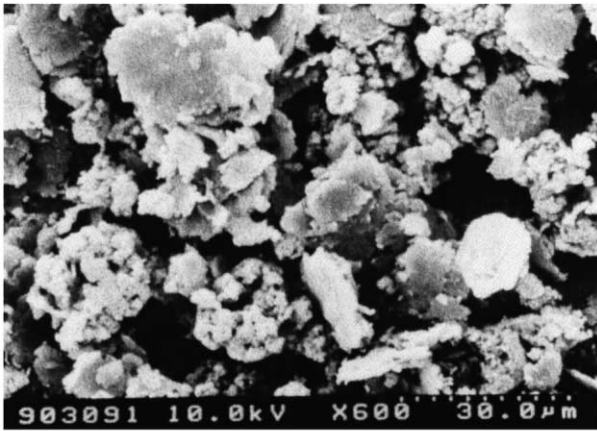
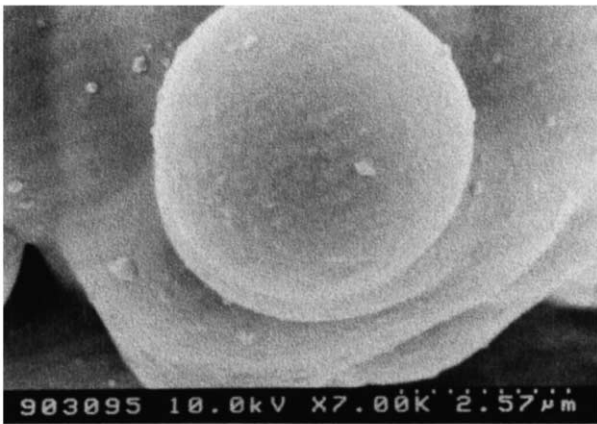


Fig. 2. FT-IR spectra for the MCPAs.



a)



b)

Fig. 3. SEM photographs of (a) PANI ($\times 600$) and (b) MCPA3 particles ($\times 7000$).

the second step corresponds to the decomposition of the backbone. As the doping state of the PANI particles increased, its thermal stability decreased. However, weight loss of MCPA is decreased due to an uncured MF resin, especially oxidative degradation of the melamine rings at 350–400°C and degradation of the residual fraction at 450°C [30].

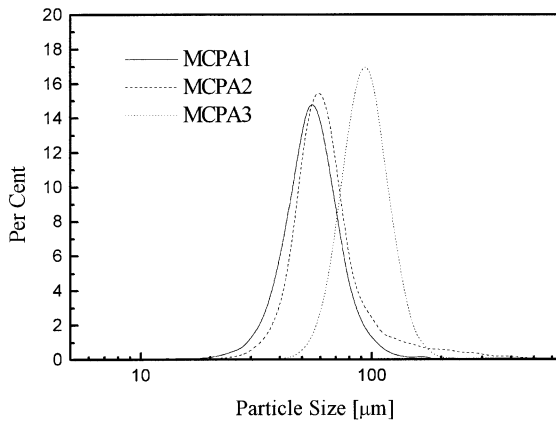


Fig. 4. Particle size distributions for the MCPA particles as a function of MF resin content.

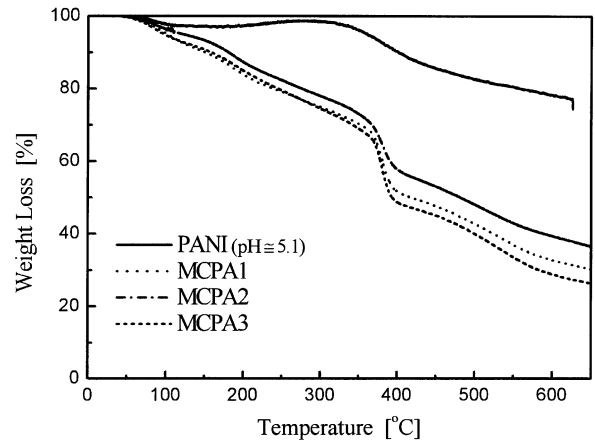


Fig. 5. TGA diagrams of the PANI and MCPA particles.

Fig. 6 shows the shear stress behavior of 20 wt% MCPA2 in silicone oil for seven different electric field strengths. This flow curve was obtained using the controlled shear rate (CSR) mode. In the absence of an electric field, the fluid behavior is similar to that of a Newtonian fluid, with the slope of one for the shear stress vs. shear rate. In addition, dynamic yield stresses, which are the shear stress at the limit of zero shear rate, were observed to increase with electric field strength. Prior to encapsulation, the pH of the PANI was approximately 5. Lee et al. [17] concluded that a PANI particles prepared at pH 5 was unable to produce ER effects, because its conductivity was too high. In this paper, the conductivity of the particles was reduced, because the MF resin enveloped outside the conducting PANI particles and played the role of an insulator by reducing the polarization force between particles. To confirm the insulation effect of the MF resin on the PANI particles, we measured the conductivity of PANI and MCPA particles. PANI particles were molded into pellets using the PANI particle by itself. However, since the MCPA particles were not easy to mold into pellets, a gum arabic (GA) was used as a binder with weight ratio of 1:2 to make pellets. The

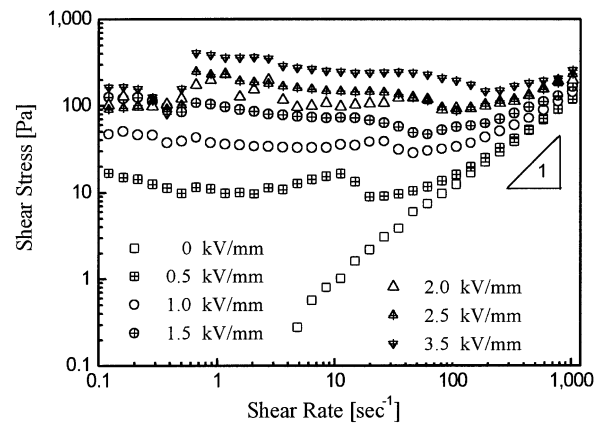


Fig. 6. Shear stress vs. shear rate measured by the CSR mode at various electric field strengths (20 wt% caPA2 in 50 cS silicone oil).

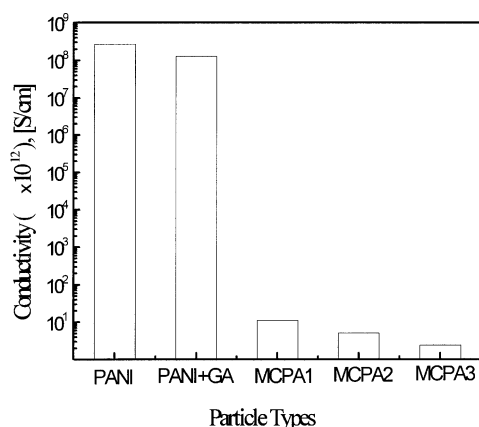


Fig. 7. Comparison of electric conductivities of PANI, PANI binded with GA (PANI + GA), and MCPAs binded with GA.

conductivity (σ) measurements are shown in Fig. 7. σ was obtained from $\sigma = d/RA$, (A is the surface area, d the thickness and R the measured resistance of the pellet). The measured σ for the PANI (pH \approx 5.1) is 2.72×10^{-4} S/cm, and that of the PANI + GA (PANI and GA mixture) 1.28×10^{-4} S/cm. Even though GA reduces the conductivity of PANI by half, the order of magnitude of PANI conductivity remains same. Therefore, adopting GA to measure the MCPA is verified to be a reasonable method, and conductivities of the GA binded MCPA1, MCPA2 and MCPA3 are 1.11×10^{-11} , 5.09×10^{-12} and 2.39×10^{-12} S/cm, respectively. This range in conductivity is the same order of magnitude to that of the conventional PANI particles obtained after the doping and dedoping process [17]. As shown in Fig. 7, MCPA1 has the highest conductivity among the three MCPAs, due to the smallest amount of the MF resin among encapsulated particles. As the MF resin amount increases, lower conductivity values are observed, showing that the wall (MF resin) thickness controls the conductivity of the PANI particles. This showed that synthesized MF resin is a good electric insulator.

Fig. 8 illustrates the effect of the amount of MF resin used for microencapsulation on static yield stress for seven different applied electric field strengths via the controlled shear stress (CSS) mode. MF resins reduced the static yield stress, and the decrease of the static yield stress as a function of the MF resin content becomes remarkable when increasing the imposed electric field strength as shown in Fig. 8(a). The correlation of the static yield stress (τ_y) and the electric field strength (E) is presented as follows:

$$\tau_y \propto E^m \quad (1)$$

The exponent, m , for the MCPAs was about 1.52 as shown in Fig. 8(b). The dependency of the yield stress on the electric field strength differs from the E^2 dependency suggested by the classic polarization model. These phenomena indicate that increasing content of MF resins influences the rheological properties and the insulation effect with applied electric field strength. Alignment of the ER fluid

particles into the characteristic fibrous structures and the increased shear resistance is believed to be due to the polarization of the particles and the resulting attractive forces among them [9]. The insulating coating increases the distance between the polarized particles and thus reduces the electrostatic interaction. The occurrence of a maximum yield stress may be attributed to surface polarization, which is determined by electron movement within the PANI particles and electron hopping between the PANI particles under a high voltage electric field [39]. When the electron movement within the PANI particles plays an important role in the surface polarization, the yield stress increases. However, when the electron hopping between the PANI particles determines the surface polarization of the PANI particles, the yield stress decreases with an increase in the content of MF resin. In addition, since we fixed a particle concentration of the ER fluids to be 20 wt%, increasing content of the MF resins will decrease slightly the volume fraction of the PANI in the core. This decrease of the PANI volume fraction is also considered to be the cause of the decreasing behavior of yield stress.

Viscoelastic properties of ER fluids arise from particle chain structures. Gamota and Filisko [40] categorized ER fluids into three regions: pre-yield, yield, and post-yield regions, exhibiting linear viscoelastic, nonlinear viscoelastic,

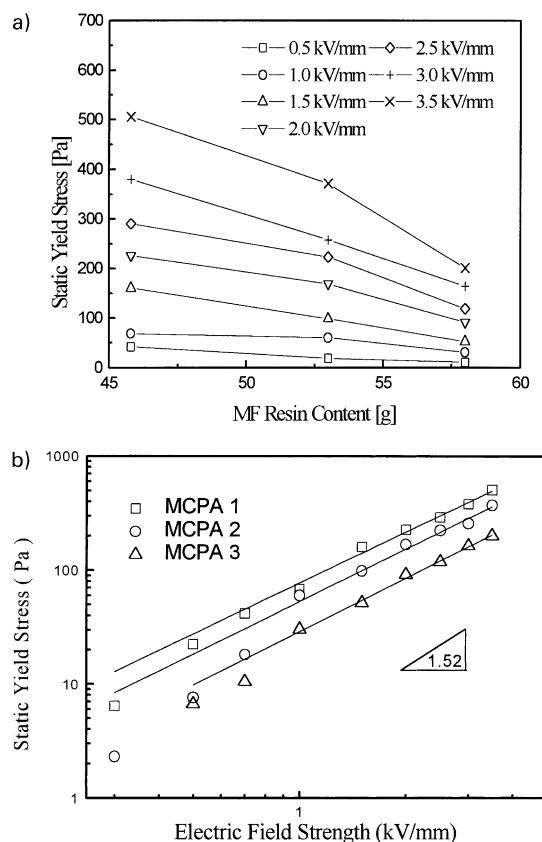


Fig. 8. Static yield stress vs. MF resin content (a) and change of static yield stress vs. electric field strength for the MCPAs (b) measured by CSS mode at seven different electric field strengths.

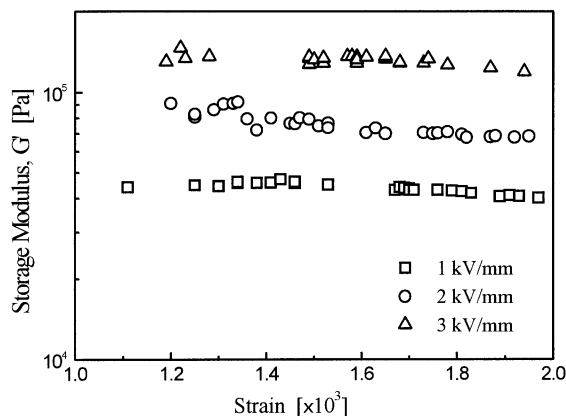


Fig. 9. G' vs. strain for an amplitude sweep at a fixed frequency of 1 Hz (20 wt% MCPA2 in silicone oil).

and plastic behavior, respectively. Furthermore, the deformations depend on the applied electric field strength, strain amplitude, and frequency.

In the dynamic test, chain structures change during deformation and also exhibit viscoelastic properties under imposed electric fields. However, it must be emphasized that the driving force for chain formation is induced electric polarization. During the chain rupture and reformation cycle, the required electric energy is continuously fed to the system to compensate for the viscous dissipation by mechanical rupture of chains [41]. Similar to the rotation test, the storage modulus (G') increases as the applied electric field strength increases. Because viscoelastic properties are mainly dominated by the particle chain structures, the state is analyzed via the rheological parameters including storage modulus, loss modulus, and loss tangent. Fig. 9 represents G' as functions of strain amplitude at a frequency (ω) of 1 Hz and electric field strength of 2 kV/mm for the MCPA2 ER fluid system. From the frequency sweep experiment, the linear viscoelastic region of the strain is determined. G' in the linear viscoelastic region increased as a function of electric field strength. In this region, the ER fluid behaves as linear viscoelastic, which is dominated by the particle chain structure in an imposed electric field. Above a certain degree of deformation, the chain structure breaks down, and the elasticity of the ER fluid abruptly decreases [40,42].

We then chose a strain of 0.002 for the frequency sweep measurement and investigated the rheological behavior as a function of frequency from 0.1 to 100 Hz. Fig. 10 shows the frequency dependence of storage modulus for a 20 wt% ER suspension with various applied electric fields. Increased plateau values of G' over three decades of frequency were also observed for dodecylbenzenesulfonic acid doped PANI-based [43] and aluminosilicate-based ER fluids [44] in imposed electric fields.

In conclusion, ER fluids consisting of the microencapsulated, conductive PANI in silicone oil were investigated. Thickness of the shell and size of MCPA particles were

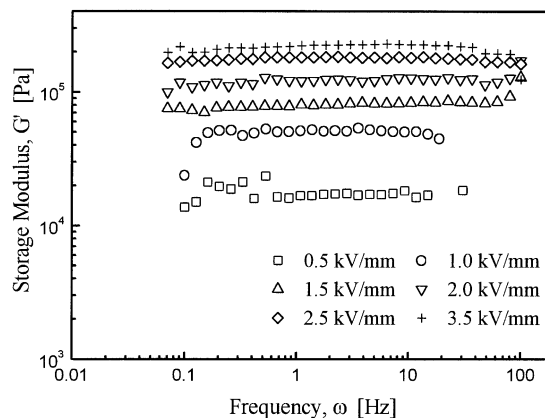


Fig. 10. G' vs. ω as a function of electric field strength (20 wt% MCPA1 in silicone oil).

controlled with the amount of the reaction reagents. These conditions affect the electric properties of PANI. The static yield stresses of the MCPAs were increased with the imposed electric field, and decreased with MF resin content. This was due to the polarization forces between the PANI particles. These phenomena were remarkably reduced by increasing the imposed electric field strength. The yield stress was also found to be proportional to approximately $E^{1.5}$ [45]. Furthermore, despite the fact that the yield stress of the microencapsulation method shows less than that of ordinary doping–dedoping system of pure polyaniline particle, this microencapsulation is observed to control the conductivity of the ER fluid without doping and dedoping steps, which are very time consuming, generally taking a week.

Acknowledgements

This work was supported by grant from the KOSEF through Applied Rheology Center at Korea University, Korea. The authors also wish to thank the referees for their valuable comments.

References

- [1] Sakurai R, See H, Saito T, Asai S, Sumita M. *Rheol Acta* 1999;38:478.
- [2] Placke P, Richert R, Fischer EW. *Colloid Polym Sci* 1995;273:848.
- [3] Jeon D, Park C, Park K. *Int J Mod Phys B* 1999;13:2221.
- [4] Wen W, Tam WY, Sheng P. *J Mater Sci Lett* 1998;17:419.
- [5] Choi HJ, Kim JW, Yoon SH, Fujiura R, Komatsu M, Jhon MS. *J Mater Sci Lett* 1999;18:1445.
- [6] Böse H. *Int J Mod Phys B* 1999;13:1878.
- [7] Cho MS, Choi HJ, Chin IJ, Ahn WS. *Micropor Mesopor Mater* 1999;32:233.
- [8] Kim SG, Choi HJ, Jhon MS. *Macromol Chem Phys* 2001 (in press).
- [9] Block H, Kelly JP. *J Phys D: Appl Phys* 1988;21:1661.
- [10] Tanaka K, Akiyama R, Takada K. *J Appl Polym Sci* 1997;66:1079.
- [11] Tanaka K, Takahashi A, Akiyama R. *Phys Rev E* 1998;58:R1234.

- [12] Choi HJ, Cho MS, Jhon MS. *Int J Mod Phys B* 1999;13:1901.
- [13] Choi HJ, Sim IS, Jhon MS. *J Mater Sci Lett* 2000;19:1629.
- [14] Gow CJ, Zukoski CF. *J Colloid Interf Sci* 1990;136:175.
- [15] Quadrat O, Stejskal J, Kratochvíl P, Klason C, McQueen D, Kubát J, Sába P. *Synth Met* 1998;97:37.
- [16] Choi HJ, Kim TW, Cho MS, Kim SG, Jhon MS. *Eur Polym J* 1997;33:699.
- [17] Lee JH, Cho MS, Choi HJ, Jhon MS. *Colloid Polym Sci* 1999;277:73.
- [18] Kim JW, Choi HJ, To K. *Polym Engng Sci* 1999;39:1493.
- [19] Choi HJ, Kim JW, To K. *Synth Met* 1999;101:697.
- [20] Cho MS, Kim TW, Choi HJ, Jhon MS. *J Macromol Sci, Pure Appl Chem* 1997;A34:901.
- [21] Cho MS, Choi HJ, To K. *Macromol Rapid Commun* 1998;19:271.
- [22] Kim JW, Kim SG, Choi HJ, Jhon MS. *Macromol Rapid Commun* 1999;20:450.
- [23] Kim BH, Jung JH, Joo J, Kim JW, Choi HJ. *J Korean Phys Soc* 2000;36:366.
- [24] Joo J, Long SM, Pouget JP, Oh EJ, MacDiarmid AG, Epstein AJ. *Phys Rev B* 1998;57:9567.
- [25] Akhavan J, Slack K, Wise V, Block H. *Int J Mod Phys B* 1999;13:1931.
- [26] Thies C. In: Benita S, editor. *Microencapsulation: methods and industrial applications*, New York: Marcel Dekker, 1996. p. 1–19.
- [27] Dietrich K, Herma H, Nastke R, Bonatz E, Teige W. *Acta Polym* 1989;40:243.
- [28] Dietrich K, Bonatz E, Geistlinger H, Herma H, Nastke R, Purz H-J, Schlawne M, Teige W. *Acta Polym* 1989;40:325.
- [29] Foris PL, Brown RW, Phillips PS. United States Patent 4 100 103; 1978.
- [30] Allen G, Bevington JC. In: Eastmond GC, Ledwith A, Russo S, Sigwalt P, editors. *Comprehensive polymer science*, vol. 5. Oxford: Pergamon Press, 1989. p. 651–4.
- [31] Cho MS, Kim JW, Choi HJ, Webber RM, Jhon MS. *Colloid Polym Sci* 2000;278:61.
- [32] Blais JF. *Amino resins*, New York: Reinhold, 1959. p. 19–20.
- [33] Ott J. In: Stoye D, Freitag W, editors. *Resins for coating: chemistry, properties, and application*, Cincinnati, OH: Hanser, 1996. p. 109–18.
- [34] Choi HJ, Lee YH, Kim CA, Jhon MS. *J Mater Sci Lett* 2000;19:533.
- [35] Choi HJ, Lee JH, Cho MS, Jhon MS. *Polym Engng Sci* 1999;39:493.
- [36] Chu SH, Lee SJ, Ahn KH. *J Rheol* 2000;44:105.
- [37] Cho MS, Choi YJ, Choi HJ, Kim SG, Jhon MS. *J Mol Liq* 1998;75:13.
- [38] Kulkarni VG, Campbell LD, Mathew WR. *Synth Met* 1989;30:321.
- [39] Xie H-Q, Guan J-G, Guo J-S. *J Appl Polym Sci* 1997;64:1641.
- [40] Gamota DR, Filisko FE. *J Rheol* 1991;35:399.
- [41] Otsubo Y, Sekine M, Katayama S. *J Rheol* 1992;36:479.
- [42] Jordan TC, Shaw MT, Mcleish TCB. *J Rheol* 1992;36:441.
- [43] Kim SG, Kim JW, Cho MS, Choi HJ, Jhon MS. *J Appl Polym Sci* 2001;79:108.
- [44] Hao T, Xu Y. *J Colloid Interf Sci* 1997;185:324.
- [45] Sim IS, Kim JW, Choi HJ, Kim CA, Jhon MS. *Chem Mater* 2001;13:1243.